



The integrated use of GPS/GLONASS observations in network code differential positioning

Paweł Przestrzelski¹ · Mieczysław Bakuła^{1,2} · Roman Galas³

Received: 31 July 2015 / Accepted: 7 July 2016 / Published online: 18 July 2016
© The Author(s) 2016. This article is published with open access at Springerlink.com

Abstract We present the methodology and results of GPS/GLONASS integration in network code differential positioning for regional coverage across Poland using single frequency. Previous studies have only concerned the GPS system and relatively short distances to reference stations of up to tens of kilometers. This study is limited to using GPS and GLONASS. However, the methodology presented applies to all satellite navigation systems. The deterministic and stochastic models, as well as the most important issues in GPS/GLONASS integration are discussed. Two weeks of the GNSS observations were processed using software developed by the first author. In addition to interpolation of pseudorange corrections (PRCs) within the polygon of reference stations, the effect of their extrapolation outside that polygon is also briefly presented. It is well known that the positioning accuracy in a network of heterogeneous receivers can be degraded by GLONASS–FDMA frequency-dependent hardware biases. Our research reveals that when using such networks, the effect of these

biases on the network differential GNSS (NDGNSS) positioning results as derived from both GPS and GLONASS can be reduced by simple down-weighting of GLONASS observations. We found that the same approach for the homogeneous equipment is not required; however, it can enhance performance of NDNSS. Yet, the addition of the down-weighted GLONASS pseudoranges still improves the positioning accuracy by 14–25 %. The representative NDNSS estimation is characterized by 0.17, 0.12 and 0.32 m RMS errors for the north, east and up component, respectively.

Keywords Pseudorange · Differential positioning · Network solution · GPS · GLONASS · GNSS

Introduction

Algorithms of classical Differential GPS (DGPS) or Differential GNSS (DGNSS) positioning are based on differential corrections to pseudoranges of the rover receiver. This is known as observation space representation. The achievable accuracy of DGPS has recently been investigated by Specht (2011) and confirmed by Przestrzelski and Bakuła (2014b) to be at a level of few decimeters. There are two basic approaches: single reference station and network of reference stations. We consider the network approach.

The network approach eliminates systematic errors associated with a spatial decorrelation and improves accuracy (Wübbena et al. 1996). Among all of the network-based DGPS systems, four groups can be distinguished depending on their operational coverage: global, continental, regional and local. Examples are WAAS (the US Wide Area Augmentation System), German SAPOS

✉ Paweł Przestrzelski
pawel.przestrzelski@uwm.edu.pl

Mieczysław Bakuła
mbakula@uwm.edu.pl

Roman Galas
roman.galas@tu-berlin.de

¹ Faculty of Geodesy, Geospatial and Civil Engineering,
University of Warmia and Mazury in Olsztyn,
Prawocheńskiego 15, 10-720 Olsztyn, Poland

² Aeronautics Faculty, Polish Air Force Academy, Dywizjonu
303, 08-521 Dęblin, Poland

³ Department of Geodesy and Geoinformation Science,
Technische Universität Berlin, Straße des 17. Juni 135,
10623 Berlin, Germany

(Satelliten POSitionierungsdienst) and OmniSTAR VBS service.

The spatial distribution of the reference stations implies a reachable accuracy for user positioning and, together with the position requirements for a particular application, determines the applicability of each DGPS system. For example, the SAPOS's service EPS (Echtzeit Positionierungs-Service or real-time positioning service) provides corrections to the GPS code measurements giving a horizontal accuracy of 0.5–3 m and vertical accuracy of 1–5 m (<http://www.sapos.de>).

In general, an accuracy of 1 m can be reached over a few hundred kilometers using DGPS and a single-frequency GPS receiver with the VBS service of the OmniSTAR active reference networks (Pérez-Ruiz et al. 2011). The European Geostationary Navigation Overlay Service (EGNOS), a European counterpart of WAAS, provides corrections and some integrity parameters to C/A code measurements on the GPS L1 frequency only and allows users to reach a meter-level accuracy or even better (Ali et al. 2012).

DGPS for local coverage has also been investigated. Nejat and Kiamehr (2013) presented numerical results of the network-based DGPS positioning in mountainous regions using various interpolation models, where the RMS error was 1.1 m or worse. It was demonstrated that the use of linear interpolation is sufficient for flat areas to improve DGPS by approximately 40 % (Oh et al. 2005) and allow the system to reach the accuracy of 0.1–0.3 m while smoothing calculated coordinates (Bakuła 2010). In these cases, the distances to reference stations were in the range of tens of kilometers. The above examples concerned GPS system only.

Decimeter–meter-level accuracy is also provided by other nationwide DGPS services using single frequency. Unfortunately, despite the declaration of high accuracy, recent research has revealed systematic errors in the performance of some services and poorer than declared positioning capabilities. For example, the position error of the KODGIS service provided by the ASG-EUPOS system exceeded the declared 0.25 m, particularly for the height component which reaches an RMS (root mean square) error of 0.83 m (Przestrzelski and Bakuła 2014a).

The aim of this study was to investigate GPS/GLONASS integration in multi-station code differential positioning in homogeneous and heterogeneous networks using single frequency. We use a network of three reference stations located across Poland and rover receivers from different manufacturers. Thus far many authors have investigated GPS/GLONASS integration in the single point positioning mode, DGNSS or precise carrier phase-based solutions, e.g., Angrisano et al. (2013), Choy et al. (2013), Pan et al. (2016), Przestrzelski and Bakuła (2014b) or

Wanninger and Wallstab-Freitag (2007). None of these investigations concerned the network code GPS/GLONASS differential solution.

Integrated use of GPS and GLONASS

The benefits of combined GPS/GLONASS positioning are well known, i.e., improved performance capabilities of the navigation system. However, adding GLONASS observations to GPS is not a straightforward process. The main problems are caused by time systems, reference frames and signal structures. The GPS-GLONASS time system difference has to be calculated per epoch as an additional unknown. By introducing a quasi-observable or pseudomeasurement, it can be considered constant in over brief time intervals or it can be predicted (Angrisano et al. 2013; Cai and Gao 2009; Zinoviev 2005). The GLONASS reference frame PZ-90.11 agrees with the International Terrestrial Reference Frame (ITRF) 2008 at the centimeter level as does the most recent realization of WGS84 (G1674). Thus, by choosing the ITRF 2008 reference frame, the conventional 7-parameter transformation can be neglected for most applications.

However, signal structure differences carry some implications. Whereas GPS signals are based on the code division multiple access (CDMA) principle, the GLONASS satellites transmit signals based on the frequency division multiple access (FDMA). New GLONASS signals are being designed and tested that will use CDMA, but for the next decade or so, GLONASS–FDMA signals will still be in use (Revnivikh 2010). Therefore, GLONASS receivers must process FDMA satellite signals, which can introduce inter-channel biases (ICBs) that cannot be canceled by differencing GLONASS observations between different types of receivers (Wanninger and Wallstab-Freitag 2007). Zinoviev (2005) stated that receivers of the same type will experience similar ICBs so that these biases can be removed to a large extent in a differential mode. We investigated this statement in our study. Furthermore, code and carrier phase ICBs differ in magnitudes and have to be discriminated (Yamada et al. 2010; Wanninger 2012). GLONASS ICBs, if not taken into account, can degrade position accuracy, and for this reason, we will compensate for its negative influence in combined GPS/GLONASS solutions by a down-weighting approach.

Mathematical model

The observation equation for the pseudoranges can be written as:

$$P_i^k(t) = \rho_i^k(t) + c[\delta_i(t) - \delta^k(t)] + I_i^k + T_i^k + d^{\text{eph}} + d_i(t) + d^k(t) + \text{mp}_i(t) + \varepsilon_i^k \tag{1}$$

where $P_i^k(t)$ is the measured pseudorange, t is the measurement epoch, $\rho_i^k(t)$ is the geometric range between the satellite k at time of signal transmission and the receiver i at time of signal reception, c is the speed of light in a vacuum, $\delta_i(t)$ is the receiver clock bias, $\delta^k(t)$ is the satellite clock bias, I_i^k is the ionospheric delay, T_i^k is the tropospheric delay, d^{eph} is the effect of broadcast ephemeris error, $d_i(t)$ is the receiver hardware delay, $d^k(t)$ is the satellite hardware delay, $\text{mp}_i(t)$ is the multipath effect and ε_i^k is the pseudorange measurement error. At this point, we do not distinguish between GPS and GLONASS observations.

Most of the biases listed in (1) can be reduced, or even canceled, by taking linear combinations of the primary observations, processing differenced observations or using models of the biases. Optionally, one can improve a bias model by estimating a correction from the data along with other unknowns, as is the case of the troposphere delay. Hardware delays, if not canceled in the differentiation method, can be calibrated. The test data used in this investigation were acquired around the maximum period of the current 11-year solar cycle. DGNSS eliminates systematic errors associated with satellites (Hofmann-Wellenhof et al. 2008) and distance-dependent errors correlated over a certain area (Seeber 2003). Please note that the uncorrelated errors such as measurement noise, multipath and hardware delays cannot be fully eliminated in DGNSS. Also, a user inherits the errors incurred at the reference station (Monteiro et al. 2005). Numerical experiments have been performed in this study in a simulated real-time approach; however, we have not analyzed PRC latencies.

In order to reduce the effects of unmodelled, correlated errors due to the distance decorrelation and partly uncorrelated errors, a linear interpolation of PRCs has been implemented using at least three reference stations (Bakuła 2010). According to Bakuła (2006), the PRCs for n reference stations generate a correlation plane for every satellite. Therefore, the PRC for a single satellite k can be presented as the following set of equations:

$$\begin{aligned} a(t)x_{\text{REF}1} + b(t)y_{\text{REF}1} + c(t) &= \text{PRC}_{\text{REF}1}^k(t) \\ a(t)x_{\text{REF}2} + b(t)y_{\text{REF}2} + c(t) &= \text{PRC}_{\text{REF}2}^k(t) \\ &\vdots \\ a(t)x_{\text{REF}n} + b(t)y_{\text{REF}n} + c(t) &= \text{PRC}_{\text{REF}n}^k(t) \end{aligned} \tag{2}$$

x_{REF} and y_{REF} are plane coordinates of the reference station. The coefficients $a(t)$, $b(t)$ and $c(t)$ are calculated for

every epoch and can be obtained using the least-squares approach:

$$\begin{bmatrix} x_{\text{REF}1} & y_{\text{REF}1} & 1 \\ x_{\text{REF}2} & y_{\text{REF}2} & 1 \\ \vdots & \vdots & \vdots \\ x_{\text{REF}n} & y_{\text{REF}n} & 1 \end{bmatrix} \begin{bmatrix} a(t) \\ b(t) \\ c(t) \end{bmatrix} = \begin{bmatrix} \text{PRC}_{\text{REF}1}^k(t) \\ \text{PRC}_{\text{REF}2}^k(t) \\ \vdots \\ \text{PRC}_{\text{REF}n}^k(t) \end{bmatrix} \tag{3}$$

The matrix form is:

$$AX = L \tag{4}$$

and the solution is as follows:

$$\hat{X} = (A^T A)^{-1} A^T L \tag{5}$$

Hence, the correction for the user receiver location can be obtained:

$$\text{PRC}_i^k(t) = \hat{a}(t)x_i + \hat{b}(t)y_i + \hat{c}(t) \tag{6}$$

where $\text{PRC}_i^k(t)$ is the interpolated pseudorange correction, x_i , y_i are the approximated plane coordinates of the rover receiver and $\hat{a}(t)$, $\hat{b}(t)$, $\hat{c}(t)$ are the estimated values of the coefficients.

We restrict our investigations to GPS and GLONASS; however, the presented formulas are suitable for all available satellite navigation systems. In order to perform the iterated, weighted, linearized least-squares (WLS) algorithm to compute the navigation solution, we need at least five pseudoranges from a mixed satellite constellation. For clarity of notation, we dropped the epoch symbol t . The number of GPS and GLONASS satellites is denoted by the superscripts kG and nR , respectively, and the partial derivatives matrix (H) has $kG + nR$ rows. In this study, the H matrix for a GPS/GLONASS position using pseudorange observations is as follows:

$$H = \begin{bmatrix} -\frac{x^{1G} - x_{i0}}{\rho_{i0}^{1G}} & -\frac{y^{1G} - y_{i0}}{\rho_{i0}^{1G}} & -\frac{z^{1G} - z_{i0}}{\rho_{i0}^{1G}} & 1 & 0 \\ \vdots & \vdots & \vdots & \vdots & \vdots \\ -\frac{x^{kG} - x_{i0}}{\rho_{i0}^{kG}} & -\frac{y^{kG} - y_{i0}}{\rho_{i0}^{kG}} & -\frac{z^{kG} - z_{i0}}{\rho_{i0}^{kG}} & 1 & 0 \\ -\frac{x^{1R} - x_{i0}}{\rho_{i0}^{1R}} & -\frac{y^{1R} - y_{i0}}{\rho_{i0}^{1R}} & -\frac{z^{1R} - z_{i0}}{\rho_{i0}^{1R}} & 0 & 1 \\ \vdots & \vdots & \vdots & \vdots & \vdots \\ -\frac{x^{nR} - x_{i0}}{\rho_{i0}^{nR}} & -\frac{y^{nR} - y_{i0}}{\rho_{i0}^{nR}} & -\frac{z^{nR} - z_{i0}}{\rho_{i0}^{nR}} & 0 & 1 \end{bmatrix} \tag{7}$$

where $x^{kG/nR}$, $y^{kG/nR}$ and $z^{kG/nR}$ are k -th GPS or n -th GLONASS satellite coordinates; x_{i0} , y_{i0} and z_{i0} are the a priori coordinates of the rover receiver and $\rho_{i0}^{kG/nR}$ is the geometric range. The columns of the matrix (7) represent

partial derivatives of geometric path distance with respect to the vector of parameters. The vector of observations for DGNSS or NDNSS is:

$$L = \begin{bmatrix} P_i^{1G} - \rho_{i0}^{1G} + \text{PRC}_i^{1G} \\ \vdots \\ P_i^{kG} - \rho_{i0}^{kG} + \text{PRC}_i^{kG} \\ P_i^{1R} - \rho_{i0}^{1R} + \text{PRC}_i^{1R} \\ \vdots \\ P_i^{nR} - \rho_{i0}^{nR} + \text{PRC}_i^{nR} \end{bmatrix} \quad (8)$$

and the vector of parameters is:

$$X = \begin{bmatrix} \Delta x \\ \Delta y \\ \Delta z \\ c\delta_i \\ c\delta_i + c\delta_{\text{GPGL}} \end{bmatrix} \quad (9)$$

Following Torre and Caporali (2015), at each epoch, we solve for station coordinates, the receiver clock bias $c\delta_i$ and the receiver clock bias plus GPS-GLONASS time offset $c\delta_i + c\delta_{\text{GPGL}}$. Alternatively, an unknown parameter $c\delta_{\text{GPGL}}$ could be estimated together with three-dimensional coordinates and the receiver clock bias $c\delta_i$. Both forms are equivalent. Similarly, other GNSS systems can be involved. Please note that no frequency-dependent bias is estimated for GLONASS. The estimator of the unknown vector of parameters is calculated as follows:

$$\hat{X} = (H^T W H)^{-1} H^T W L \quad (10)$$

where W is the weight matrix of observations,

$$W = \text{diag}[\sigma^{-2}, \sigma^{-2}, \dots, \sigma^{-2}] \quad (11)$$

Let us denote F^s and w^{kS} as the satellite system error factor and the weight function of the satellite system s and satellite k , respectively. Then, the diagonal elements of (11) are expressed as:

$$\sigma^2 = F^S (w^{kS})^2 \quad (12)$$

The elevation-dependent (elev) weight function w implemented in the PRSolve application, which is a part of the GPS Tool Kit (GPSTk) project (Tolman et al. 2004), has been applied in this study to down-weight satellites at low elevations:

$$w = \begin{cases} 1 & \text{if elev} \geq 30^\circ \\ \frac{\sin \text{elev}}{\sin 30^\circ} & \text{if elev} < 30^\circ \end{cases} \quad (13)$$

The threshold value 30° was determined empirically. An elevation-dependent sine-weighting model can be applied

instead. The function given in (13) allows for a smooth transition of weights, whereas simple sine-weighting automatically assigns at least a two times lower weight for a satellite just below 30° .

Research description

The research was conducted using an application written in C++ programming language, compiled with gcc 4.8 and supported by Code::Block 13.12 programming environment. The software is based on the GPSTk project in version 2.4. Some other resources such as GeographicLib and Essential GNSS were also used. The application has been prepared under LINUX operating system and follows the open source idea.

The CORS stations presented in Fig. 1 and marked with filled symbols were chosen to evaluate the solution. They are part of the TPI NETpro system operating in Poland. For this experiment, the reference stations BOLE, BRAN and NARO were selected as regional test reference network. The distances between the three reference stations are 452, 508 and 559 km, respectively. Eight other stations of the

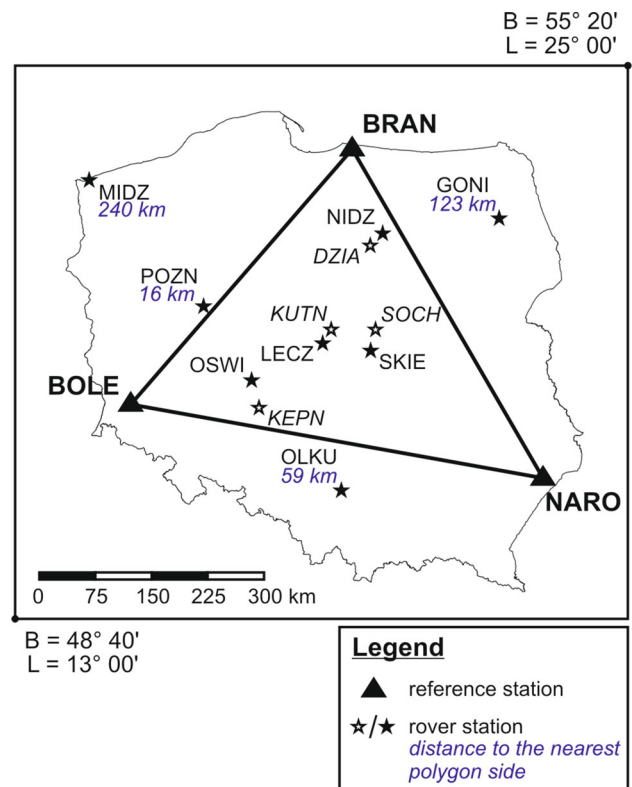


Fig. 1 Distribution of stations over the territory of Poland. The filled and open symbols denote Topcon and Trimble equipment, respectively. The distances of stations outside the network polygon are indicated relative to the nearest polygon side

TPI NETpro network were selected as rover stations. The stations LECZ, NIDZ, OSWI and SKIE are located inside the regional test network polygon; GONI, MIDZ, OLKU and POZN are outside. The TPI NETpro stations used in this study are equipped with a Topcon NET-G3A receiver and a Topcon CR-G5 antenna forming a set of homogeneous GNSS equipment.

The stations DZIA, KEPN, KUTN and SOCH presented in Fig. 1 with open symbols are a part of the ASG-EUPOS network. They are equipped with a Trimble NetR9 receiver and a TRM59900.00 antenna except SOCH which used a NetR5 receiver and a TRM57971.00 antenna. We used them to evaluate the effects of ICB on heterogeneous equipment in the NDGNSS positioning mode. Knowing the precise coordinates of all GNSS stations, which are given in the European Terrestrial Reference Frame (ETRF) 2000, allows for simple and direct estimation of the accuracy of the algorithms presented. We transformed the benchmark coordinates from ETRF 2000 to ITRF 2008 using an application provided by the EUREF Permanent Network Central Bureau (http://www.epncb.oma.be/_productsservices/coord_trans/).

The GNSS data were post-processed following the processing strategy presented in Table 1 and Fig. 2. Two weeks of data between DOY 352 and 365 of 2014 were randomly selected to produce a large sample size. Daily RINEX (Receiver Independent Exchange Format) files were post-processed on an epoch-by-epoch basis using the developed software. In order to obtain the best positioning results, we smoothed noisy pseudoranges using the Hatch filter (Hatch 1982). Differences relative to the benchmark coordinates were computed, transformed from ITRF 2008 and analyzed in the local north, east and up (N, E and U) system for each site. The UTM (Universal Transverse Mercator) coordinate system with a central meridian at 19° has been used in this study as x , y plane coordinates in (2).

Table 1 Selected parameter settings of the GNSS data processing

Parameter	Characteristic
Observations	GPS and GLONASS pseudoranges at L1 (C/A)
Interval	30 s
Elevation cutoff angle	15°
Smoothing	carrier-smoothing using L1
Observation weight function	Equation (13)
Satellite system error factor (F^s)	1 for GPS, 2 for GLONASS
Satellite orbits	broadcast
Time span	14 days
Receiver antenna model	none

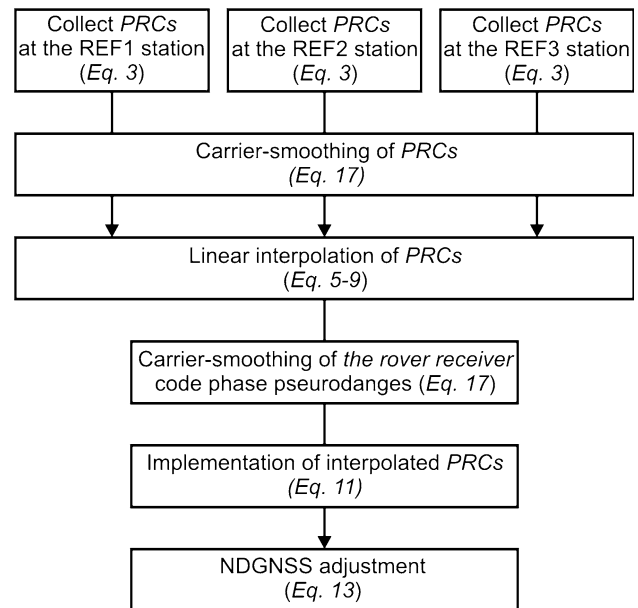


Fig. 2 Data flow scheme for the NDGNSS positioning

Data quality

We investigated residual errors of corrected pseudoranges and values of multipath effects for all rover stations on DOY 352. It is a representative day; abnormal performances were not observed during the experiment. Unmodelled errors for corrected pseudoranges of LECZ and KUTN are presented in Figs. 3 and 4. The stations represent the homogeneous and heterogeneous group, respectively, and they are located near the middle of the network polygon. The top panels show daily time series of residuals for GPS and GLONASS satellites. One color represents one satellite. The bottom panels show the mean values of residuals for each satellite individually. The GPS mean residuals are given in blue, whereas GLONASS satellites were marked with different colors by their frequency number.

Better quality of GPS observations compared to GLONASS can be observed in both cases: for the homogeneous in Fig. 3 (left versus right panels) and heterogeneous GNSS equipment in Fig. 4 (left versus right panels). This feature is especially obvious for KUTN where the mean daily residuals for individual GLONASS satellites deviate more from the reference value. Please note that mean daily residuals have similar magnitudes and signs for GLONASS satellites with the same frequency number, e.g., GLONASS PRN numbers 2 and 6, or 20 and 24. It is characteristic for the heterogeneous group investigated in this study and may indicate the existence of a frequency-dependent bias.

More details on residuals are given in Tables 2 and 3. These tables contain average value, mean absolute error

Fig. 3 LECZ daily time series and mean values of observation residuals on DOY 352 for GPS (left panels) and GLONASS (right panels) satellites

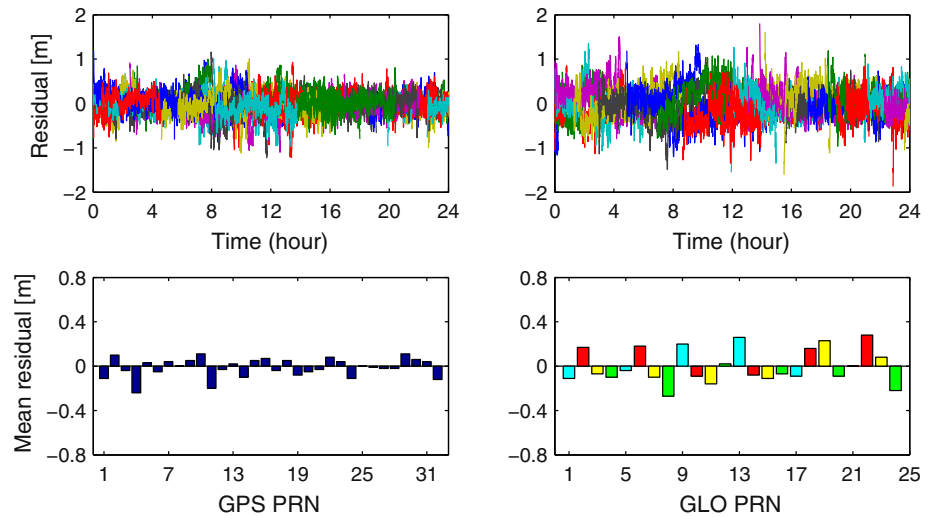


Fig. 4 KUTN daily time series and mean values of observation residuals on DOY 352 for GPS (left panels) and GLONASS (right panels) satellites

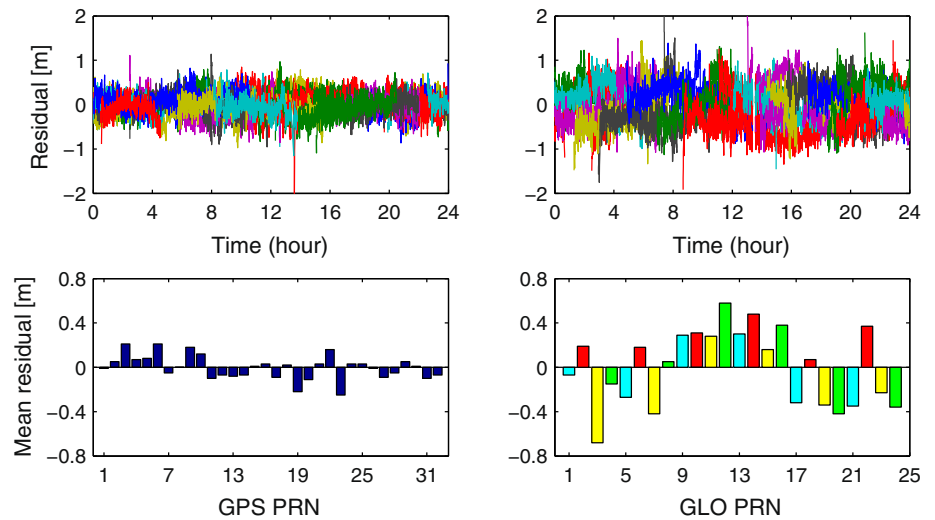


Table 2 Statistics on residuals of GPS and GLONASS observations of TPI NETpro stations

Satellite system	Statistic	Station name							
		GONI	LECZ	MIDZ	NIDZ	OLKU	OSWI	POZN	SKIE
GPS	Average	0.00	-0.01	0.00	-0.01	0.00	0.01	-0.01	-0.01
	MAE	0.07	0.07	0.06	0.06	0.06	0.06	0.03	0.06
	σ	0.34	0.23	0.33	0.28	0.26	0.25	0.28	0.27
	Max	2.71	1.22	2.02	2.06	1.65	2.59	1.68	1.82
GLO	Average	0.00	0.00	0.00	-0.01	0.00	0.00	0.00	0.00
	MAE	0.36	0.13	0.21	0.23	0.22	0.13	0.12	0.08
	σ	0.43	0.29	0.41	0.36	0.32	0.29	0.33	0.32
	Max	3.20	1.87	3.49	3.23	1.89	1.94	2.22	2.36

Values are given in meters

(MAE), standard deviation (σ) and maximum value of observation residuals for all GPS and GLONASS satellites.

It can be seen that the precision (σ) of GPS and GLONASS observations is similar in both groups of GNSS equipment, with better precision and lower maximum

Table 3 Statistics on residuals of GPS and GLONASS observations of ASG-EUPOS stations

Satellite system	Statistic	Station name			
		DZIA	KEPN	KUTN	SOCH
GPS	Average	-0.01	0.00	-0.01	0.00
	MAE	0.08	0.10	0.09	0.06
	σ	0.23	0.23	0.21	0.24
	Max	1.60	1.79	2.66	3.12
GLO	Average	0.00	0.00	0.00	0.00
	MAE	0.21	0.27	0.30	0.32
	σ	0.30	0.29	0.27	0.32
	Max	2.71	2.87	2.58	3.34

Values are given in meters

residuals for the GPS system. Please note that the average values of residuals at all stations for GPS and GLONASS are all near 0.00 m, while significant MAE values for GLONASS indicate the presence of systematic errors. Despite the fact of using the same type of GNSS equipment in the homogeneous group of receivers, some systematic errors are present at GONI, MIDZ, NIDZ and OLKU (Table 2).

The differences in the RMS values given are mainly caused by the multipath effect occurring at a particular site. It is a factor significantly affecting DGNSS/NDGNSS positioning results. The values of the multipath error for code measurements were computed and investigated using MP1 formulas given in Rocken et al. (1995). Tables 4 and 5 contain mean MP1 values for three satellite constellations from DOY 352, a representative day. Multipath is a station-dependent error that changes slowly with time; thus, one multipath error for code measurements over 1 day is sufficient for this investigation. Differences between the lowest and highest MP1 values for TPI NETpro stations reached up to 0.20, 0.48 and 0.35 m for the GPS, GLONASS and combined GPS/GLONASS constellation, respectively. For ASG-EUPOS stations, these differences were up to a few centimeters. SOCH is an exception, but it used a different receiver and antenna model.

These results are consistent with assertions of Cai et al. (2015) who reported that the code multipath and noise level for GLONASS are the largest of all GNSS

Table 4 Mean MP1 values for TPI NETpro stations on DOY 352

Satellite constellation	Station name							
	GONI	LECZ	MIDZ	NIDZ	OLKU	OSWI	POZN	SKIE
GPS	0.37	0.21	0.26	0.31	0.17	0.24	0.29	0.35
GLONASS	0.89	0.43	0.53	0.66	0.41	0.49	0.69	0.74
Combined	0.65	0.33	0.41	0.50	0.30	0.38	0.50	0.56

Values are given in meters

Table 5 Mean MP1 values for ASG-EUPOS stations on DOY 352

Satellite constellation	Station name			
	DZIA	KEPN	KUTN	SOCH
GPS	0.26	0.27	0.27	0.31
GLONASS	0.46	0.46	0.43	0.60
Combined	0.37	0.37	0.36	0.49

Values are given in meters

systems. TPI NETpro antennas are usually mounted on rooftops, as is the case of our experiment, which can cause discrepancies in values of the code multipath among stations.

Evaluating the effects of ICB on heterogeneous equipment in NDNSS positioning

Four pairs of closely spaced rover stations were selected to examine the effects of homogeneous versus heterogeneous equipment of rovers. These four pairs are LECZ/KUTN, NIDZ/DZIA, OSWI/KEPN and SKIE/SOCH and are equipped with Topcon/Trimble, respectively. Recall that the reference stations were equipped with Topcon sets. Data from DOY 352 were used to study these effects. The observations were processed in three variants of the processing strategy: NDGPS, and NDNSS with ($F^R = 2$), and without ($F^R = 1$) down-weighting GLONASS observations. Down-weighting of GLONASS observations by a factor of 2 is a common practice (Pan et al. 2016; Wanninger and Wallstab-Freitag 2007) because they are affected by ICBs, which cannot be eliminated in the differential mode. However, Choy et al. (2013) state that deweighting the GLONASS pseudorange observations allows their residuals to absorb the neglected inter-hardware code bias.

Table 6 contains the positioning accuracy results and the increase rate parameter (Inc.) which provides the percentage increase/decrease in NDNSS accuracy compared to NDGPS. The results were grouped according to homogeneity of the GNSS equipment at the reference and rover stations. Positioning errors for NDGPS are similar in both groups, while this is not true for the NDNSS solutions.

We have found that the change of the satellite system error factor F^R to 1 for GLONASS observations in the case of homogeneous equipment randomly affects the positioning results of the GNSS solution, but does not decrease the accuracy (Inc. ≥ 0 %). The same operation for the heterogeneous receiver/antenna sets causes the accuracy to decrease (Inc. < 0 %), whereas setting $F^R = 2$ positively affects the positioning accuracy achieved in both groups. This may be due to the presence of frequency-dependent biases in GLONASS observations. A significantly increased number of satellites improved the constellation geometry which translates into the accuracy improvement despite the weight reduction in GLONASS observations (Fig. 5).

Positioning inside and outside the network polygon

In order to assess accuracy of network code differential GPS/GLONASS positioning, we used data gathered between DOY 352 and 365. It is well known that the best positioning results using network solutions can be

obtained, while corrections are being interpolated. LECZ, NIDZ, OSWI and SKIE stations were used to evaluate the NDGNSS positioning algorithms inside the network polygon. Rover stations are spread out within the triangle created by three reference stations: BOLE, BRAN and NARO. These seven stations formed a homogeneous equipment set.

Figure 6 presents the NDGPS and NDGNSS time series for LECZ. Once again this station is used as a representative station. Please note the different scales for N/E components and the U component. The figure is scaled such that outliers are not plotted. This is not significant for the discussion that follows. Horizontal dashed lines help one to recognize that most of the NDGNSS N/E estimates for LECZ did not exceed ± 0.5 m for 99.58/99.96 % of the time, and that most of the height estimates were within ± 1.0 m for 99.91 % of the time. Moreover, 95.51, 98.86 and 88.33 % of LECZ NDGNSS positions fall within ± 0.3 m for the N, E and U components. Use of GPS+GLONASS mitigates maximum deviations and improves the positioning accuracy (Table 7). Outliers given in the table could be reduced by applying Kalman

Table 6 RMS errors of the network code differential positioning with various GLONASS satellite system error factors (F^R) on DOY 352

GNSS equipment	Station name		$F^R = 2$			$F^R = 1$	
			NDGPS (m)	NDGNSS (m)	Inc. (%)	NDGNSS (m)	Inc. (%)
Homogeneous	LECZ	N	0.24	0.17	29	0.17	29
		E	0.16	0.13	19	0.14	13
		U	0.40	0.32	20	0.32	20
	NIDZ	N	0.25	0.21	16	0.23	8
		E	0.18	0.16	11	0.18	0
		U	0.51	0.44	14	0.49	4
	OSWI	N	0.23	0.18	22	0.18	22
		E	0.14	0.12	14	0.13	7
		U	0.38	0.33	13	0.35	8
	SKIE	N	0.30	0.22	27	0.20	33
		E	0.19	0.15	21	0.14	26
		U	0.44	0.36	18	0.35	20
Heterogeneous	DZIA	N	0.28	0.20	29	0.19	32
		E	0.19	0.17	11	0.20	-5
		U	0.45	0.36	20	0.41	9
	KEPN	N	0.24	0.21	13	0.27	-13
		E	0.18	0.18	0	0.21	-17
		U	0.40	0.34	15	0.42	-5
	KUTN	N	0.25	0.19	24	0.22	12
		E	0.17	0.17	0	0.22	-29
		U	0.41	0.33	20	0.44	-7
	SOCH	N	0.34	0.27	21	0.30	12
		E	0.22	0.22	0	0.26	-18
		U	0.53	0.47	11	0.54	-2

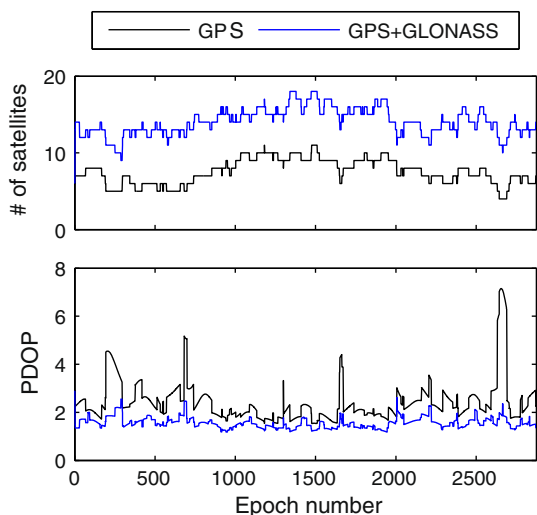


Fig. 5 Number of satellites and PDOP values of GPS and GPS/GLONASS constellations (DOY 352)

filtering, receiver autonomous integrity monitoring (RAIM) algorithms or modifying the stochastic model. This will be investigated in the near future.

Based on formulas given in Przechodzinski and Bakula (2014b), the RMS errors, standard deviations (STD) and Δ parameters were calculated. Δ is a difference of RMS and STD. It allows us to detect the presence of systematic errors in the estimated coordinates. It takes only positive values, and $\Delta > 0.00$ m should be interpreted as the occurrence of a systematic error; however, it does not indicate the number of errors that occurred.

The average NDGNSS positioning errors from DOYs 352–365 for the four selected stations were 0.19, 0.14 and 0.36 m. OSWI was characterized by the lowest RMS errors, i.e., 0.17, 0.12 and 0.32 m for the N, E and U components, respectively. The Δ parameter for NDGPS/NDGNSS was always near zero, which means that systematic errors were almost eliminated (Fig. 7). Residual

Fig. 6 NDGPS (black) and NDGNSS (green) positioning residuals of LECZ on DOY 352–365/2014

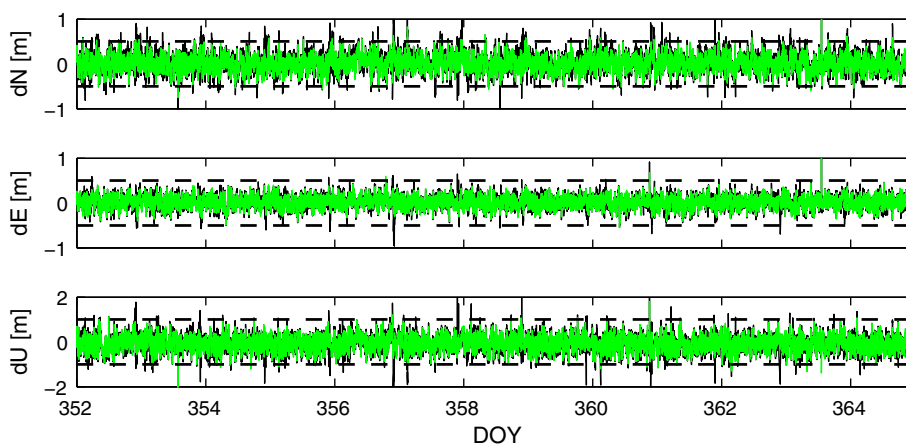


Table 7 Detailed statistics for LECZ obtained on DOYs 352–365

	NDGPS			NDGNSS		
	N	E	U	N	E	U
RMS	0.23	0.15	0.40	0.17	0.13	0.33
Average	0.03	0.02	-0.07	0.01	0.02	-0.07
Min	-2.59	-0.96	-7.03	-1.04	-0.57	-4.81
Max	7.51	2.76	2.63	2.27	1.08	1.79

Values are given in meters

systematic errors are associated with long distances to the reference stations.

Every network-based system has to deal with areas which are outside its coverage. GONI (123 km), MIDZ (240 km), OLKU (59 km) and POZN (16 km) were selected to act as rovers for this purpose. The values in parentheses indicate how far each site is from the network polygon.

PRCs extrapolation improved the position estimates for POZN and OLKU to a similar extent as was seen for the sites in the interpolation tests. However, extrapolation resulted in a worse positioning performance for the two more distant stations GONI and MIDZ. This is especially visible for the U component where minor systematic errors can be observed (Fig. 8). Unfortunately, these results are suspect because anomalies caused repeated restart and re-initialization at GONI and MIDZ somewhere around 4:30 local time each day. We were not able to identify a reason for this recurring situation. The results shown were produced by removing 2 min of measurements after the re-initialization. While this enabled processing to be completed, and the results shown for the sake of completeness, it also raises questions about these results. This issue, PRCs extrapolation and other issues are the topics of further research.

Table 8 summarizes the positioning accuracy obtained from eight rover stations during 2 weeks of the experiment.

Fig. 7 RMS and Δ values of NDGPS (left panels) and NDGNSS (right panels) for interpolation positioning results

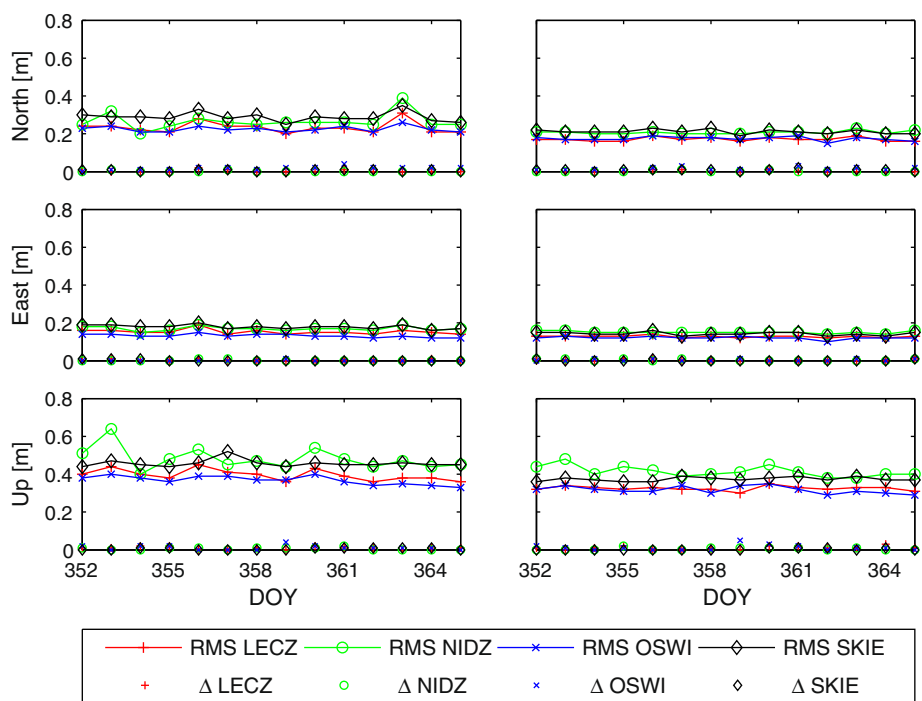
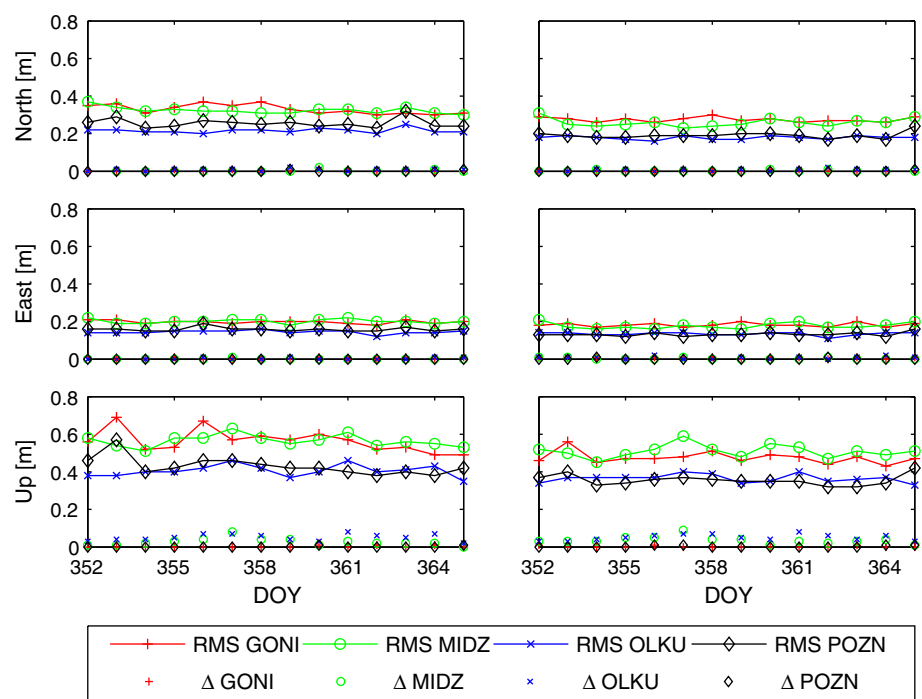


Fig. 8 RMS and Δ values of NDGPS (left panels) and NDGNSS (right panels) for extrapolation positioning results



Overall, the combination of GPS and GLONASS pseudoranges improved the position estimation over GPS only for the interpolated/extrapolated group by 25/20, 14/11 and 16/13 % for the N, E and U components, respectively. The two extrapolation test stations located near the network polygon, i.e., OLKU and POZN, were improved in the NDGNSS mode by 23, 13 and 13 % for N, E and U components.

Summary and conclusion

We have presented the methodology of and the results for NDGNSS positioning that provides regional coverage with a few decimeters accuracy. The research revealed that using heterogeneous GNSS equipment, the negative impact of ICBs on NDGNSS positioning results can be reduced by simple down-weighting GLONASS observations without

Table 8 Final RMS errors for DOYs 352–365/2014 of the interpolated and extrapolated stations

Solution		Interpolation				Extrapolation			
		LECZ	NIDZ	OSWI	SKIE	GONI	MIDZ	OLKU	POZN
NDGPS	N	0.23	0.27	0.22	0.29	0.33	0.33	0.22	0.26
	E	0.15	0.17	0.13	0.18	0.20	0.20	0.14	0.16
	U	0.40	0.48	0.37	0.46	0.56	0.57	0.41	0.43
NDGNSS	N	0.17	0.21	0.17	0.21	0.28	0.26	0.18	0.19
	E	0.13	0.15	0.12	0.14	0.18	0.18	0.13	0.13
	U	0.33	0.41	0.32	0.37	0.48	0.51	0.37	0.36

Values are given in meters

degrading the accuracy. We found that the same approach for the homogeneous equipment is not required; however, it can enhance performance of NDGNSS. The addition of down-weighted GLONASS observations in the homogeneous group improved the positioning accuracy of NDGPS by 14–25 %, with the best positioning accuracy in these tests being 0.17, 0.12 and 0.32 m RMS errors for the *N*, *E* and *U* components, respectively.

The case of extrapolated stations has shown that the applicability of the solution is not limited to rovers within the network polygon formed by the reference stations. POZN and OLKU, which are 16 km and 59 km outside the network polygon, respectively, reached similar positioning accuracy as the test stations inside the polygon. However, as could be expected, more the distant stations GONI and MIDZ, 123 km and 240 km outside the polygon, were degraded, particularly in height showing minor systematic errors. We note that other issues at these distant sites might also have affected the results. Residual systematic errors could be mitigated using other interpolation methods or by taking into account the station height in computations.

Despite some imperfections, the multi-station DGNSS approach provided a positioning accuracy, as described by the RMS error, of a few decimeters using only pseudorange and carrier phase L1 observations. The purpose of the carrier phase observations merely was smoothing of the pseudoranges. Future investigations will require preservation of the positioning accuracy on an epoch-by-epoch basis and will concern static and kinematic measurements in urban areas.

Acknowledgments The authors acknowledge the anonymous reviewers for carefully reading the manuscript and providing constructive feedback, and the TPI company and members of the Advanced Methods for Satellite Positioning Laboratory for providing data. This research was supported by the Deutscher Akademischer Austausch Dienst (DAAD) scholarship for Ph.D. students and by the project “Scholarships for Ph.D. students of Podlaskie Voivodeship” co-financed by European Social Fund, Polish Government and Podlaskie Voivodeship.

Open Access This article is distributed under the terms of the Creative Commons Attribution 4.0 International License (<http://creativecommons.org/licenses/by/4.0/>), which permits unrestricted use, distribution, and reproduction in any medium, provided you give appropriate credit to the original author(s) and the source, provide a link to the Creative Commons license, and indicate if changes were made.

creativecommons.org/licenses/by/4.0/), which permits unrestricted use, distribution, and reproduction in any medium, provided you give appropriate credit to the original author(s) and the source, provide a link to the Creative Commons license, and indicate if changes were made.

References

- Ali K, Pini M, Dosis F (2012) Measured performance of the application of EGNOS in the road traffic sector. *GPS Solut* 16(2):135–145. doi:[10.1007/s10291-011-0253-5](https://doi.org/10.1007/s10291-011-0253-5)
- Angrisano A, Gaglione S, Gioia C (2013) Performance assessment of GPS/GLONASS single point positioning in an urban environment. *Acta Geod Geophys* 48(2):149–161. doi:[10.1007/s40328-012-0010-4](https://doi.org/10.1007/s40328-012-0010-4)
- Bakuła M (2006) An approach of network code differential GPS positioning for medium and long distances. *Artificial Satellites* 41(4):137–148. doi:[10.2478/v10018-007-0012-6](https://doi.org/10.2478/v10018-007-0012-6)
- Bakuła M (2010) Network code DGPS positioning and reliable estimation of position accuracy. *Surv Rev* 42(315):82–91. doi:[10.1179/003962610X12572516251448](https://doi.org/10.1179/003962610X12572516251448)
- Cai C, Gao Y (2009) A combined GPS/GLONASS navigation algorithm for use with limited satellite visibility. *J Navigation* 62(4):671–685. doi:[10.1017/S0373463309990154](https://doi.org/10.1017/S0373463309990154)
- Cai C, He C, Santerre R, Pan L, Cui X, Zhu J (2015) A comparative analysis of measurement noise and multipath for four constellations: GPS, BeiDou, GLONASS and Galileo. *Surv Rev*. doi:[10.1179/1752270615Y.0000000032](https://doi.org/10.1179/1752270615Y.0000000032)
- Choy S, Zhang S, Lahaye F, Héroux P (2013) A comparison between GPS-only and combined GPS + GLONASS Precise Point Positioning. *J Spat Sci* 58(2):169–190. doi:[10.1080/14498596.2013.808164](https://doi.org/10.1080/14498596.2013.808164)
- Hatch R (1982) The synergism of GPS code and carrier measurements. Proceedings of the international geodetic symposium on satellite doppler positioning. Las Cruces, New Mexico, pp 1213–1231
- Hofmann-Wellenhof B, Lichtenegger H, Wasle E (2008) GNSS—GPS, GLONASS, Galileo and more. Springer, Vienna
- Monteiro LS, Moore T, Hill C (2005) What is the accuracy of DGPS? *J Navigation* 58(2):207–225. doi:[10.1017/S037346330500322X](https://doi.org/10.1017/S037346330500322X)
- Nejat D, Kiamehr R (2013) An investigation on accuracy of DGPS network-based positioning in mountainous regions, a case study in Alborz network. *Acta Geod Geophys* 48(1):39–51. doi:[10.1007/s40328-012-0003-3](https://doi.org/10.1007/s40328-012-0003-3)
- Oh KR, Kim JC, Nam GW (2005) Development of navigation algorithm to improve position accuracy by using multi-DGPS reference stations’ PRC information. *J Global Position Syst* 4(1–2):144–150

- Pan L, Cai C, Santerre R, Zhang X (2016) Performance evaluation of single-frequency point positioning with GPS, GLONASS BeiDou and Galileo. *Surv Rev*. doi:[10.1080/00396265.2016.1151628](https://doi.org/10.1080/00396265.2016.1151628)
- Pérez-Ruiz M, Carballido J, Agüera J, Gil JA (2011) Assessing GNSS correction signals for assisted guidance systems in agricultural vehicles. *Precision Agric* 12(5):639–652. doi:[10.1007/s11119-010-9211-4](https://doi.org/10.1007/s11119-010-9211-4)
- Przeźrzelski P, Bakula M (2014a) Performance of real-time network code DGPS services of ASG-EUPOS in north-eastern Poland. *Technical Sciences* 17(3):191–207
- Przeźrzelski P, Bakula M (2014b) Study of differential code GPS/GLONASS positioning. *Annual of Navigation* 21:117–132. doi:[10.1515/aon-2015-0010](https://doi.org/10.1515/aon-2015-0010)
- Revnivykh S. (2010) GLONASS Status and Progress. Proc. ION GNSS 2010, Institute of Navigation, Portland, Oregon, September, pp 609–633
- Rocken C, Meertens C, Stephens B, Braun J, Vanhove T, Perry S, Ruud O, McCallum M, Richardson J (1995) UNAVCO Academic Research Infrastructure (ARI) Receiver and Antenna Test Report. Technical report, UNAVCO, Boulder, CO
- Seeber G (2003) *Satellite geodesy: foundations, methods and applications*. Walter de Gruyter, Berlin
- Specht C (2011) Accuracy and coverage of the modernized Polish Maritime differential GPS system. *Adv Space Res* 47(2):221–228. doi:[10.1016/j.asr.2010.05.021](https://doi.org/10.1016/j.asr.2010.05.021)
- Tolman BW, Harris RB, Gaussiran T, Munton D, Little J, Mach R, Nelsen S, Renfro B, Schlossberg D (2004) The GPS Toolkit—Open Source GPS Software. Proc. ION GNSS 2004, Institute of Navigation, Long Beach, California, September, pp 2044–2053
- Torre AD, Caporali A (2015) An analysis of intersystem biases for multi-GNSS positioning. *GPS Solut* 19(2):297–307. doi:[10.1007/s10291-014-0388-2](https://doi.org/10.1007/s10291-014-0388-2)
- Wanninger L (2012) Carrier-phase inter-frequency biases of GLONASS receivers. *J Geodesy* 86(2):139–148. doi:[10.1007/s00190-011-0502-y](https://doi.org/10.1007/s00190-011-0502-y)
- Wanninger L, Wallstab-Freitag S (2007) Combined processing of GPS, GLONASS, and SBAS code phase and carrier phase measurements. Proc. ION GNSS 2007, Institute of Navigation, Fort Worth, Texas, September, pp 866–875
- Wübbena G, Bagge A, Seeber G, Böder V, Hankemeier P (1996) Reducing Distance Dependent Errors for Real-Time Precise DGPS Applications by Establishing Reference Station Networks. Proc. ION GPS 1996, Institute of Navigation, Kansas City, Missouri, September, pp 1845–1852
- Yamada H, Takasu T, Kubo N, Yasuda A (2010) Evaluation and calibration of receiver inter-channel biases for RTK-GPS/GLONASS. Proc. ION GNSS 2010, Institute of Navigation, Portland, Oregon, September, pp 1580–1587
- Zinoviev AE (2005) Using GLONASS in combined GNSS receivers: current status. Proc. ION GNSS 2005, Institute of Navigation, Long Beach, California, September, pp 1046–1057



Paweł Przeźrzelski graduated from the University of Warmia and Mazury (UWM) in Olsztyn, Poland, in 2011. He is a Ph.D. student at the Department of Satellite Geodesy and Navigation of UWM in Olsztyn. His research interests cover algorithms and software development for GNSS positioning in obstructed areas and precise navigation.



Mieczysław Bakula is an Associate Professor at the Department of Satellite Geodesy and Navigation of the University of Warmia and Mazury in Olsztyn, Poland. His research is focused on GNSS positioning, advanced data processing and network adjustments. Since 2011, he is involved in precise navigation at the Polish Air Force Academy in Dęblin, Poland.



GNSS and integrated GNSS/INS positioning and navigation.

Roman Galas has graduated from the Technical University of Warsaw in Astronomical and Physical Geodesy. From 1985 to 1987, he was Alexander von Humboldt Fellow. He also worked at various Universities and research institutes, i.e., Technical University Munich, University of Bonn and the GeoForschungsZentrum Potsdam (GFZ). Since 2008, he is Professor at the Technical University Berlin. His current research interests are precise